Published in Photonics East, Boston, MA, November 2001.

New Models for Optical MEMS

Timothy P. Kurzweg[a], Jose A. Martinez[a], Steven P. Levitan[*a], Philippe J. Marchand[b], Donald M. Chiarulli[c]

[a]Department of Electrical Engineering, University of Pittsburgh

[b]Optical Micro Machines, San Diego, CA 92121

[c]Department of Computer Science, University of Pittsburgh

ABSTRACT

Computer Aided Design (CAD) tools for modeling optical MEM systems must not only model three distinct domains (optical, electrical, and mechanical), these tools must also model the interactions between the signals of these domains. We strive to create system-level models that are applicable for an optical MEM CAD tool using techniques that support accurate results and interactive computation times. This paper discusses our modeling efforts for multi-domain optical MEM systems with the implementation of these models into our CAD framework, Chatoyant. As an example of our mixed-modeling research, we present the simulation and analysis of a 2x2 optical cross connect using Chatoyant. The simulations include the dynamic response of a mechanical beam, diffractive optical effects, and the interaction between these domains.

Keywords: MEMS CAD, optical MEMS, MOEMS, OMEMS, modeling, system-level simulation

1. INTRODUCTION

In order to support the design of mixed-signal optical MEM (micro-electro-mechanical) systems, computer aided design tools must be capable of modeling, electronics, electrostatics, mechanics, guided wave optics, and free space optics. The design tools must directly support the interactions between models in all these domains, and characterize the behavior of the resulting system in an interactive environment. Obviously, CAD tools exist in each of these specialized domains and it is unnecessary to re-invent these tools. For example, SPICE is the standard simulation technique for electrical circuits and devices. Code V and ASAP are available for accurate optical modeling, and CAD tools for conventional MEMS are being designed in both academia and industry, including those by CMU[21], Microcosm[19], and MEMScaP[18]. However, these tools do not provide a single multi-domain design environment, which is needed for modeling mixed-technology applications.

This paper concentrates on the system-level modeling and simulation of optical MEM systems, focusing particularly on the models used for optical, electrical, and mechanical signals and components, which are appropriate for a mixed-signal, interactive CAD tool. Our interest is in modeling system behavior in a single integrated framework. The remainder of this paper is organized as follows. In the next section, we present an overview of previous work related to mixed-signal system-level modeling and an introduction to our optical MEM system-level simulator, Chatoyant. We then introduce our modeling techniques for the three domains that encompass optical MEM systems; first the optical, followed by a description of the piecewise linear technique that is suitable for both electrical and micro-mechanical signals and devices. Through simulating a 2x2 optical switch in Chatoyant, we show the interaction of these signals and our system-level simulation and analysis techniques.

2. SYSTEM-LEVEL MIXED-TECHNOLOGY SIMULATION

2.1. Mixed Signal, Multi Domain Simulation

The need to support modeling of various technology domains in an optical MEM design leads us to evaluate the impact of having heterogeneous signals in a common simulation framework. An optical MEM design environment needs to support electronic, mechanical, and optical components, with the possibility of extensions to other domains, such as thermal, chemical, and RF. Not only do we have to characterize the sets of interactions between components of different technologies, we also have to consider the performance of the simulation environment, which depends on the simulation method and the type of signal characterization chosen.

* Correspondence: Email: steve@ee.pitt.edu; WWW: http://kona.ee.pitt.edu/pittcad; Telephone: 412 648 9663; Fax: 412 624 8003

Several research efforts have been conducted to offer a suitable methodology for the simulation of these systems. They can be classified into two different approaches: behavioral modeling and equivalent circuit methods. Behavioral modeling is a flexible and general methodology that allows hierarchical support and mixed signal simulation. Hardware description languages with extensions to support analog signals such as VHDL-AMS or Verilog-A are used to describe the system. In this approach, the degree of abstraction obtained with the hardware description language simplifies the designer's task for the description of the system. A mixed signal CAD tool is used as the simulation framework. Consequently, the support for co-simulation is already in place. This methodology is applied in the simulation of optical MEM systems in [20].

Even though the behavioral modeling approach appears to be a promising option for the modeling of mixed-signal, multi-domain systems, it is necessary to clarify the difficulties and limitations present in this technique. During the description of the system the designer must specify the relations that define the interaction between the different signals in the system. The definition of these relationships is an active area of research today. It involves the characterization of ports, defined as transducers (energy conversion devices), and elements, defined as actuators (unidirectional energy flow devices), as explained in [24]. Additionally, this technique relies on the abstraction levels offered by the mixed-simulation framework and in doing so, it shares its drawbacks as well. For example, mixed-signal, multi-domain micro-systems consisting of a large number of elements result in large computation load.

The second approach for modeling mixed-signal multi-domain systems is based on finding an electrical equivalent representation for the non-electrical domain required to be simulated. The electrical equivalent can be simulated using any of the well known and established circuit simulators (e.g., SPICE, SABER, iSMILE[30]). This method has been used in [9,27] for the simulation of micro mechanical devices, where a mapping of these devices to a SPICE netlist is proposed. In [30], Yang simulates optoelectronic interconnection links using iSMILE as the circuit simulator engine. The limitations of this technique are the lack of support for hierarchical design and co-simulation. Because the simulation is coupled to an analog simulator, digital simulation is not supported.

The advantage of traditional circuit simulators, based on numerical integration solvers, is that they provide good accuracy when solving the linear and non-linear differential equation (DE) systems. The problems associated with these circuit simulators are their reliability and long computation times. It is also well known that there are non-convergence problems faced during simulation of electronic circuits [13]. These techniques become computationally expensive with increasing size of the network being analyzed and when the network has a high degree of non-linearity. The use of such a computationally intense algorithm as the core for an interactive CAD tool would make this solution inefficient.

Both of these approaches lack some critical aspects that we desire in our optical MEM system-level CAD tool. Neither of these approaches give an accurate representation of the optical signal as it propagates through a system. This representation is required for system-level optical MEM CAD tools, since it is often the optical signal that holds information which lead to analyses, such as BER (bit error rate), insertion loss, and data dependent crosstalk.

Before we present the details of our modeling techniques, we first introduce our system-level CAD framework in which these models are implemented.

2.2. Mixed-Signal Micro-Optical-Electro-Mechanical Simulation Tool: Chatoyant

The modeling methods presented in this paper have been implemented in our mixed-technology simulator Chatoyant. Chatoyant is a multi-level, multi-domain CAD tool that has been successfully used to design and simulate free space optoelectronic interconnect systems [14,16]. Static simulations analyze mechanical tolerancing, power loss, insertion loss, and crosstalk, while dynamic simulations are used to analyze data streams with techniques such as noise analysis and bit error rate (BER) estimation.

A Chatoyant schematic of a free-space 1x2 optical MEM cross-connect is shown in Figure 1. In Chatoyant, each icon represents a component model with sets of parameters defining the characteristics of the component. Each line represents a signal path (either optical, mechanical, or electrical) connecting the outputs of one component to the inputs of the next. This system shows an optical fiber emitting light into a free space medium. The light then travels through a collimating lens and is reflected off of a switching mirror, into the path of one of the outgoing fibers. Each optical path contains a second collimating lens, which focuses the light into the corresponding outgoing fiber. The mirror is assembled on an anchored cantilever beam, which bends into and out of the optical path by electrostatic attraction between the beam and the substrate. Three electrostatic

forces are placed on the beam/mirror icon; on the *x* and *z* positions and a torque around the *z* axis. Above the schematic, we show an optical intensity distribution as light strikes one of the outgoing fibers, while, on the right of the figure, we show a dynamic waveform and eye-diagram from a data signal being passed through the switch. Details of this system are given during a full analysis of the system toward the end of this paper.

Our approach for modeling mixed-signal, multi-domain systems is a discrete event driven simulation model, which operates over the global system. An object-oriented framework, Ptolemy[2] is used to provide this degree of abstraction for the simulation of such systems. We choose the "Dynamic Data Flow" (DDF) Ptolemy simulation method as our discrete event engine. Timing information is added to support multiple and run-time-rate variable streams of data flowing through the system. In this model of computation, the simulation scheduler creates a dynamic schedule based on the flow of data between the modules. This allows modeling of multi-dynamic systems where every component can alter the rate of consumed/produced data at any time during simulation. The scheduler also provides the system with buffering capability. This allows the system to keep track of all the signals arriving at one module when multiple input streams of data are involved.

To maximize our modeling flexibility, our signals are composite types, representing the attributes of force, displacement, velocity, and acceleration for mechanical signals, voltages and impedances for electronic signals, and wavefront, phase, orientation, and intensity for optical signals. The composite type is extensible, allowing us to add new signal characteristics as needed. Mixed-signal, multi-domain systems in Chatoyant have a conceptual and abstract representation consisting of a set of modules interchanging information. However, this simulation approach brings the challenge of developing the circuit/component modeling techniques that will be optimal for fast and accurate characterization of the different modules involved in this system. This challenge is the focus of the remainder of this paper.

In the next three sections, we introduce our optical modeling technique and our piecewise linear modeling technique that has been implemented for both electrical and mechanical models in Chatoyant.

3. OPTICAL PROPAGATION MODELING

To achieve our goal of interactive, system-level optical MEM modeling, we require the simulations to run as fast as possible, while giving accurate results to the user. Ray, or geometric, optics are the simplest of the optical propagation methods, and correspondingly have the smallest computation time. However, ray tracing has no inherent support for the optical characteristics of light. This is improved by using Gaussian optics, which satisfies the paraxial Helmholtz equation in solving for optical parameters such as waist size, depth of focus, intensity, and phase, meeting the criteria which are required for modeling optical MEM systems. An additional benefit of using Gaussian analysis is that we can approximate the behavior of the lasers used in these systems as sources of Gaussian shaped beams. The Gaussian method is quick to solve, since no explicit integration is needed to calculate the resulting Gaussian beam at the interface to adjacent components[26]. The computational complexity for both Gaussian and ray optic models is on the order of the number of beams that are being propagated. Therefore, for macro-systems, Chatoyant's support is based on the Gaussian modeling technique[16]. However, modeling optical diffraction is a

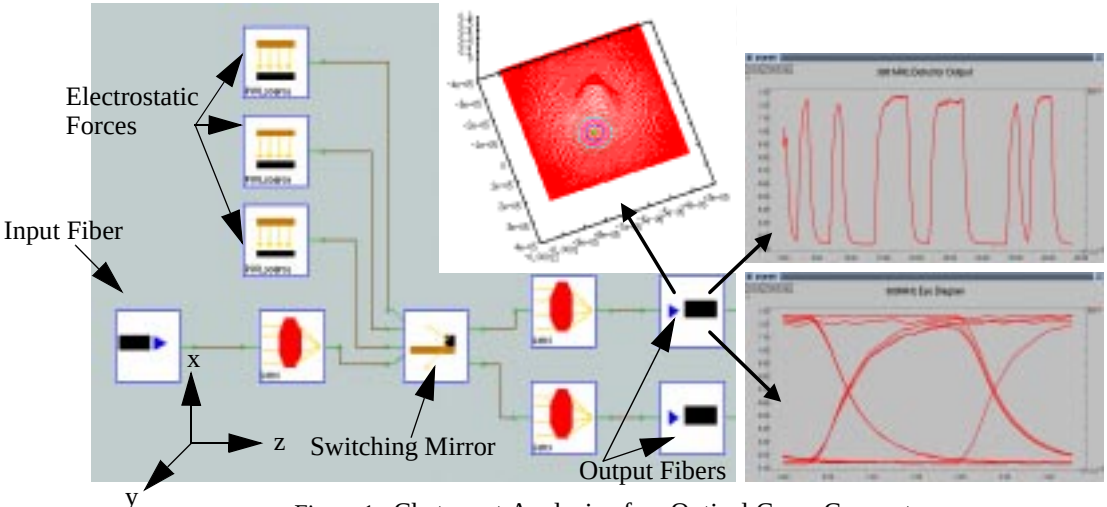

Figure 1: Chatoyant Analysis of an Optical Cross Connect

requirement for simulating optical MEM systems, due to diffractive components (i.e., gratings, binary lenses) which compose these systems. Additionally, the component sizes and distances of propagation found in these systems cause diffraction effects even in systems composed completely of refractive components. Therefore, we need to consider appropriate optical propagation methods which can meet this objective without sacrificing simulation speed.

After a study of many of the typical optical MEM systems, we have determined that a more rigorous scalar diffraction model, such as the Rayleigh-Sommerfeld scalar formulation, must be used to model light for optical MEM systems [15]. Common diffractive propagation techniques, such as the Fraunhofer and Fresnel approximations, have been found to be invalid for the small propagation distances appropriate for optical MEM systems. On the other hand, the Rayleigh-Sommerfeld formulation is only limited by having both the propagation distance and the aperture size be "greater" than the wavelength of light. Therefore, with propagation distances in valid ranges (10-1000 μm), and the ability to model the required optical characteristics, we believe that the Rayleigh-Sommerfeld formulation is the appropriate optical propagation method to use for the modeling and simulation of optical MEM systems.

However, we must evaluate the computation efficiency of this method to ensure our system-level CAD requirements is also satisfied. This is done by examining the required integration of the Rayleigh-Sommerfeld [8]:

$$U(x, y) = \frac{z}{j\lambda}\iint_A U(\xi, \eta)\frac{e^{jkr}}{r}d\xi d\eta ,$$

where, k is $2\pi/\lambda$, r is the distance from the source point (ξ,η) to the observation point (x,y), z is the distance propagated, A is the aperture area, and U is the complex optical wave function. This equation mathematically describes the Huygens-Fresnel principle in rectangular coordinates, where each point on the aperture plane is a source of spherical waves[10]. This results in the requirement that U for each point in the observation plane be calculated through the superposition of all the input sources.

The computation time of this scalar technique is therefore based on the gridding of both the aperture and observation plane. For each grid point in the observation plane, $U(x,y)$, a double integration is performed over the grid points in the aperture plane, $U(\xi,\eta)$. This is costly in computation time, however, several optimizations can be performed. First, computation time can be saved by decreasing the number of grid points used to represent the complex wave function, at a cost of accuracy. Second, in systems with radial symmetry, the integration can be reduced to a single integral. Finally, the choice of the integration algorithm effects the total computation time.

We have found the Gaussian quadrature integration method [1] to be both accurate and efficient for solving the Rayleigh-Sommerfeld integration [15]. It is well known that quadrature integration techniques offer the optimum estimate of the exact integration solution for a specific number of points (N). However, the accuracy of this method is dependent of the smoothness of the integrated function, since the function is effectively interpolated by a polynomial of degree 2N+1. In the Rayleigh-Sommerfeld expression, the possible causes of high order (i.e., "non-smooth") effects are found at the interactions of the complex wave function at the finite boundaries of the apertures. The Gaussian quadrature method will result in an accurate solution if the discontinuities in the wave function at the boundaries are negligible. This condition is satisfied by the Rayleigh-Sommerfeld initial assumption that the aperture size is larger that the wavelength of the light.

As an example of the application of the optimized Gaussian quadrature integration technique for diffraction computation, we show Chatoyant's Rayleigh-Sommerfeld simulation results of a 850 nm plane wave, passing through a 50 μm aperture, and striking a 200 μm observation plane in Figure 2. We compare our simulations with a 80x80 grid-point "base case" from MathCAD, which uses a Romberg integration technique. The table included in Figure 2 shows the computation time and relative error of the system (compared with the base case) for different grid spacing. We can see that the simulation that takes 2 hours using a Romberg algorithm can be reduced to approximately 4.5 minutes using our optimized Gaussian quadrature integration technique. The relative RMS error of this method compared to the base case is only 0.6%. As can be seen, the user can choose to reduce Chatoyant's simulation time even further at a cost of accuracy in the result.

We next examine the piece-wise linear technique that is used as a backbone for both our electrical and mechanical modeling.

4. ELECTRICAL MODELING

We propose a piece-wise linear (PWL) technique as the basis for analog simulation in a system-level framework. Additionally, if the input signals are linearized, the transfer function for the system can be obtained explicitly. This methodology

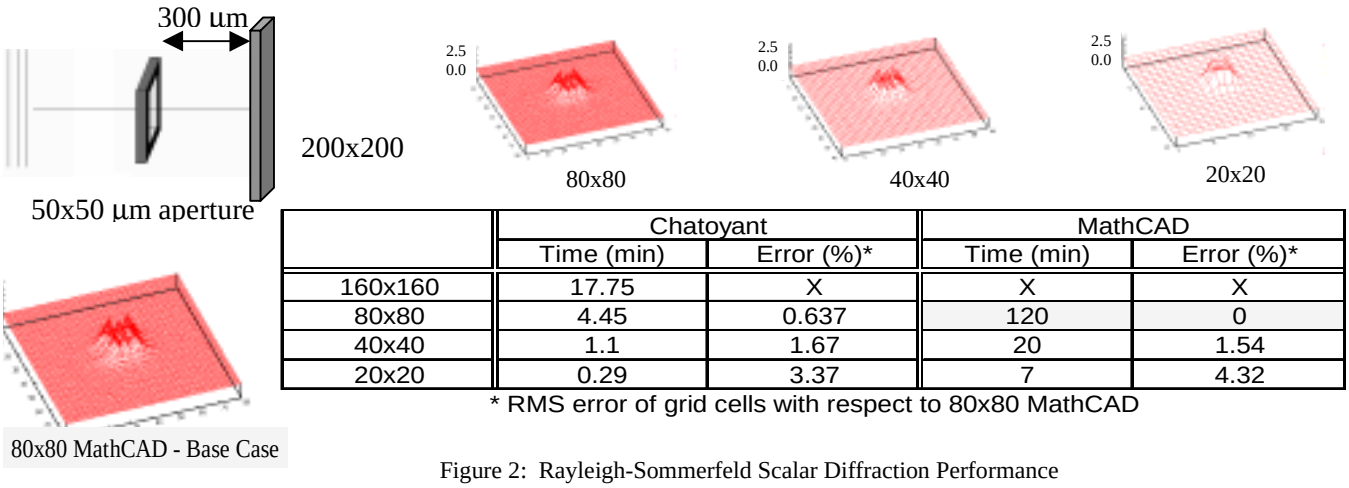

	Chatoyant		MathCAD	
	Time (min)	Error (%)*	Time (min)	Error (%)*
160x160	17.75	X	X	X
80x80	4.45	0.637	120	0
40x40	1.1	1.67	20	1.54
20x20	0.29	3.37	7	4.32

* RMS error of grid cells with respect to 80x80 MathCAD

Figure 2: Rayleigh-Sommerfeld Scalar Diffraction Performance

decreases the computational requirements by avoiding the integration process required in the conventional algorithms.

Conventional PWL numerical solvers use a superset model where ideal switches are used to switch between the PWL representations for a component into a single system model [11]. In order to avoid this computational overhead of using a superset model, we use a direct representation for the system as the PWL mathematical representation. In our case, the different configurations of the system are used corresponding to the change of regions of operation over individual non-linear components and not through ideal switches. Boundary conditions of individual non-linear components are used to determine the switching behavior between configurations. The fact that the node density is moderate for the networks generated for the modeling of opto-electro-mechanical devices in a modular environment allows us to consider piecewise linear modeling merged with linear numerical analysis as a way to achieve the desired accuracy with low computation demands.

We present an example of lumped device modeling in the electrical domain through the diagram in Figure 3(a). In the first step, we perform linear and non-linear sub-block decomposition of the circuit model representation of the device. This decomposes the design into a linear multi-port sub-block section and non-linear sub-blocks. The linear multi-port sub-block can be thought of as characterizing the interconnection network and parasitic elements while the non-linear sub-blocks characterize active non-linear behaviors.

In the second step, Modified Nodal Analysis (MNA)[6] is used to create a mathematical representation for the devices, shown in Figure 3(b). In this expression, M corresponds to the memory matrix of the system, also called the susceptance matrix, R is the conductance matrix, x is the vector of state variables, B and E are connectivity matrices, u is the excitation vector, and the y vector contains the desired variables to evaluate.

The linear elements can be directly mapped to this representation, but the non-linear elements need to first undergo a further transformation. We perform piecewise modeling of the active devices for each non-linear sub-block. When we form each

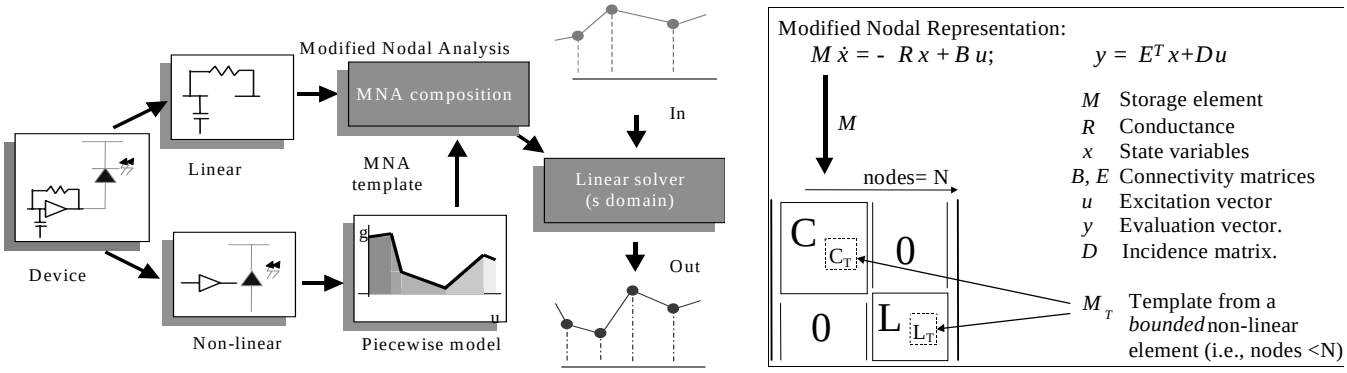

Figure 3: (a) Piecewise Modeling Technique (b) MNA Representation and Template Integration

non-linear sub-block, a MNA template is used for each device in the network. The use of piecewise models is based on the ability to change these models for the active devices depending on the changes in conditions in the circuit, and thus the regions of operation.

The templates generated can be integrated to the general MNA containing the linear components adding their matrix contents to their corresponding counterparts. This process is shown in Figure 3(b) for the storage, or memory, matrix *M*, which is composed of the capacitive matrix, *C*, and the inductive matrix, *L*. This same composition is done for the other matrices. The size of each of the template matrices is bounded by the number of nodes connected to the non-linear element.

Once the integrated MNA is formed, a linear analysis in the frequency domain can be performed to obtain the solution of the system. Constraining the signals in the system to be piecewise linear in nature allows us to use a simple transformation to the time domain without the use of costly numerical integration. For a better understanding of our modeling technique, we next present some details of the modified nodal analysis representation.

4.1. Global Mathematical Representation of the Linear Time-invariant System: MNA

We have chosen MNA as the technique to map the linear electrical network representation into a system of first-order differential equations and algebraic equations. For a development of this technique the reader can explore the work presented in [7] and [28]. This formulation, shown in Figure 3, is based in the application of the KCL (Kirchoff's current law) over the nodal representation of the circuit and the use of the state variable definition $x = \begin{pmatrix} v \\ i \end{pmatrix}$. In this state definition, $v \in \Re^n$ corresponds to the vector of voltage nodes in the network and $i \in \Re^m$ corresponds to a vector representing only the currents going through inductors, and sources in the network. What is accomplished with this state definition is a transformation from a second order ordinary differential equation problem (ODE) to a first order differential equation, at the expense of increasing the range of the linear problem from *n* to *(n+m)*.

A useful feature of this representation is that the relative inclusion of any discrete element (i.e., R, C, L, and sources) can be expressed as a pattern or "template". As mentioned previously, each element type can be described as a set of specific *R*, *M*, and *B* matrices. This set, or template, can then be used to introduce the element into the global MNA, requiring only its position in terms of a nodal index.

4.2. Time Domain Evaluation Formulation

In our technique, time evaluation of the PWL modeling is accomplished through an inverse Laplace evaluation approach, due to the benefits that this methodology offers. This technique consists of solving the system in the frequency domain and then using the inverse Laplace transform to obtain the time domain response. Inverse Laplace evaluation techniques are applicable for stiff systems and can perform well even when the system is in the presence of discontinuities in their functions [28]. Additionally, the methodology is robust to inconsistent initial condition situations. These properties result in stable techniques that do not face many of the convergence problems that affect the direct evaluation techniques.

The piecewise linear characterization is our approach to avoid the use of the integration-based formulations and the stability problems associated with them. Restricting the type of signals in the system to be PWL gives us an explicit time domain conversion expression that is the basis for our evaluation algorithm [17].

4.3. Example: PWL Modeling of the Non-Linear I-V Characteristic of a VCSEL

To show how our PWL technique applies for an opto-electronic component, the modeling of a VCSEL is presented. Typical L-I and V-I diagrams for a VCSEL are shown in the Figure 4 (a) [5]. The segmented curve represents the relation between voltage and current in the device, and the solid curve is the relation between the optical power generated by the VCSEL versus the electrical current consumed. The optical output of VCSEL devices is a non-linear function, as can been seen in Figure 4 (a). The current in the laser must surpass a threshold value to begin the lasing process. After this, the optical power production reaches a maximum value and then decreases with further increases in electrical current. The reason for this behavior is the loss of efficiency in the laser, caused by the increase in temperature as a consequence of the ohmic losses [12].

A simple two linear segment model can be used to represent the I-V curve. Because these curves are frequently produced from experimental data, the development should be based on the curve fitting of two linear segments over the data as it is shown in Figure 4 (b) [5]. Independent of the methodology used for the fitting, a result of the following form will be obtained:

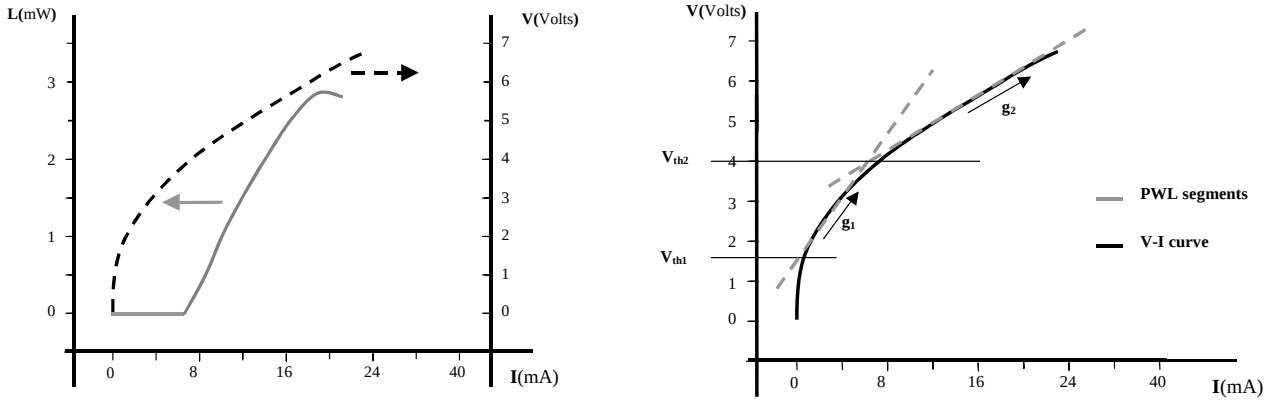

Figure 4: (a) L-I and V-I Curves for a VCSEL(35) (b) V-I Curve with PWL Model Functions

$$I_{VCSELpwl} = \begin{cases} g_2 V - I_2 & V > V_{th2} \\ g_1 V - I_1 & V_{th1} < V < V_{th2} \\ 0 & V < V_{th1} \end{cases} \qquad \begin{aligned} I_1 &= g_1 V_{th1} \\ I_2 &= g_2 V_{th2} - g_1 (V_{th2} - V_{th1}) \end{aligned}$$

The values of I_1 and I_2 are necessary to maintain continuity of values at the transition points. g_1 and g_2 correspond to the slope of the curve at the chosen transition points (V_{th1} and V_{th2}) according to the selected fitting procedure criteria.

It is interesting to note that the PWL model derived in both regions corresponds to a conductance, *g*, in parallel to a fixed current source of value *I*. This is equivalent to the widely used model of a resistance, *Rs*, in series to a voltage source, V_{th}, because these are complementary circuits.

The PWL template for each region of operation share the same generic form:

$$M = \begin{array}{c} \begin{matrix} v^a & v^b \end{matrix} \\ \begin{bmatrix} C_v & C_v \\ -C_v & C_v \end{bmatrix} \begin{matrix} v^a \\ v^b \end{matrix} \end{array} \qquad R = \begin{array}{c} \begin{matrix} v^a & v^b \end{matrix} \\ \begin{bmatrix} g & -g \\ -g & g \end{bmatrix} \begin{matrix} v^a \\ v^b \end{matrix} \end{array} \qquad B = \begin{array}{c} \begin{matrix} v^a & v^b \end{matrix} \\ \begin{bmatrix} I & -I \end{bmatrix} u^v \end{array}$$

g and *I* correspond to the pair (g_1,I_1) for region 1 and (g_2,I_2) for region 2. Indexes of *a* and *b* have been chosen relative to the positive and negative terminal of the VCSEL. A capacitor of value C_v has been added to the PWL models to account for the frequency response behavior of the VCSEL. The use of this capacitor is a normal practice in VCSEL characterization.

There is a novel concept in this template. That is, the modification of the matrix *B*, or source connectivity. The reason for this modification is the presence in the model of a constant current source of value I_1 or I_2 depending on the PWL region. To include a current source in an MNA representation a new element is added to the vector of the system *u* (u^v in this template). Additionally, the matrix *B* must reflect the inclusion of this new element according to its polarity. The value of the source can be carried in the *u* vector definition or in the *B* matrix. In this work, we have chosen to keep the *u* vector with unit values and modified the *B* matrix with the magnitude of the sources. Templates for independent sources, such as these, can be found in [17].

Additional discrete elements to characterize the wiring connections between the laser and the driver, and the frequency dependent behavior of the device can be added to complement the final electrical model. A wiring connection between the VCSEL and the external electrical driver circuit is usually characterized by a parasitic inductance value and a parasitic capacitance to ground. As described above, there is no need to create a different template to the one already developed. The addition of the bonding connections or any additional electrical circuits can be easily accomplished by adding the new elements to the network, which defines the circuit to be simulated. In our implementation of the PWL technique this is simply accomplished by adding the elements to the netlist for the device.

The advantage of this characterization is that the designer can directly simulate the effect of electrical conditions in the VCSEL or associated driver circuit against the optical power produced by this device. Additional variable dependencies can be added to the V-I VCSEL model following this approach (e.g., temperature, spot size, and threshold) that allow one to study their effect over complete systems. As shown in [17], the VCSEL model is used to examine the dependency of the temperature in which the device is operated.

For the complete modeling of the VCSEL, the same technique is also used for additional non-linear characteristics, such as the L-I curve. This is presented in [17] and is not included here for space considerations.

5. MECHANICAL MODELS

In the field of MEM modeling, there has been an increasing amount of work that uses a set of Ordinary Differential Equations (ODEs) to characterize MEM devices [27]. ODE modeling is performed over techniques such as finite element (FE) analysis, to reduce the time and amount of computational resources necessary for simulation. The model uses non-linear differential equations in multiple degrees of freedom and in mixed domains. Our technique models a MEM device by characterizing its different basic components such as beams, plate-masses, joints, and electrostatic gaps, and by using local interactions between components.

Our approach to modeling mechanical elements is to reduce the mechanical ODE representation to a form matching the electronic counterpart, seen previously. This enables the use of our same piecewise linear techniques for the mechanical models as for simulating the dynamic behavior of electrical systems.

With damping forces proportional to the velocity, the equation of motion for a mechanical structure with viscous damping effects is [23]:

$$F = KU + BV + MA$$

where, K is the stiffness matrix, U is the displacement vector, B is the damping matrix, V is the velocity vector, M is the mass matrix, A is the acceleration vector, and F is the vector of external forces affecting the structure. Obviously, knowing that the velocity is the first derivative and the acceleration is the second derivative of the displacement, the above equation can be recast to:

$$F = KU + BU' + MU''$$

Similar to the electrical modeling case, this equation represents a set of linear ODEs if the characteristic matrices K, B, and M are static and independent of the dynamics in the body. If the matrixes are not static and independent (e.g., the case of aerodynamic load effects), they represent a set of non-linear ODEs.

To reduce the above equation to a standard form, we use a modification of Duncan's reduction technique for vibration analysis in damped structural systems [4]. This modification allows the above general mechanical motion equation to be reduced to a standard first order form, similar to electrical equation found in Figure 3, which gives a complete characterization of a mechanical system.

$$\begin{bmatrix} 0 & M \\ M & B \end{bmatrix} \begin{bmatrix} U'' \\ U' \end{bmatrix} + \begin{bmatrix} -M & 0 \\ 0 & K \end{bmatrix} \begin{bmatrix} U' \\ U \end{bmatrix} = \begin{bmatrix} 0 \\ I \end{bmatrix} F$$

Using substitutions, the above equation is rewritten as:

$MbX' + MkX = EF$, where the new state variable vector $X = \begin{bmatrix} U'' \\ U' \end{bmatrix}$

Each mechanical element (beam, plate, etc.) is characterized by a template consisting of the set of matrices Mb and Mk, composed of matrices B, M, and K in the specified form seen above. If the dimensional displacements are constrained to be small and the shear deformations are ignored, the derivation of Mb and Mk is simplified and independent of the state variables in the system. Multi-node idealization can be performed by combining basic elements (e.g., two nodes) to characterize higher order modes.

Typically, this element is only a part of a bigger device made from individual components that are characterized using similar

expressions. The generalization of the previous case to an assembly of elements or mechanical structures is fairly straightforward. The general expression, seen above, characterizes the whole structure defined by a set of nodes, from which every individual element shares a subset. The next step, similar to the previously considered electronic case, is merging the individual templates together, composing the general matrix representation for the composed structure. However, a common coordinate reference must be used for this characterization of mechanical structures, since every template or element is characterized in a local reference system. The process of translation of these local templates to the global reference system can be described by:

$$S_G = A^T S_L A$$

where, A represents the translation matrix from local displacements to global displacements (a function of the structure's geometry), S_L represents the local template, and S_G is the corresponding global representation. The next step is the addition of these global representations into the general matrix form, using the matrices' nodal indexes as reference. Finally, the piecewise linear solver can be used on the composed system's general matrix.

The use of a PWL general solver for mechanical simulation decreases the computational task and allows for a trade-off between accuracy and speed. The additional advantage of using the same technique to characterize electrical and mechanical models allows us to easily merge both technologies in complex devices that interact in mixed domains.

6. SIMULATION OF 2X2 OPTICAL MEM SWITCH

To demonstrate the modeling and simulation of mixed-domain systems in a single framework, we present the modeling and simulation of a 2x2 optical MEM switch. The architecture of this switch consists of a set of four optical fibers in the shape of a "+" sign, with the input and output fibers facing each other through a free-space gap. The switching system is in the "cross" state when the light is passed straight across the free-space gap. However, to switch to the "bar" state, a micro-mirror is inserted between the fibers at a 45-degree angle, and the light is reflected to the alternate output. These two cases are shown in Figure 5.

For the simulations presented in this paper, we use a switching system based on an experimental system designed and tested at UCLA [3]. Similar to that system, a mirror is placed on top of a long anchored cantilever beam. In our system, the bar state is achieved in the steady-state of the system, with the mirror positioned between the fibers in the free-space gap. The cross state is achieved by the cantilever beam bending towards the substrate, moving the attached mirror out of the optical path. The beam movement is a result of electrostatic attraction between the substrate (with an applied voltage) and the cantilever beam. This attraction results in forces being applied to the beam.

For simplicity, we simulate only a single input switching to either the cross or bar state throughout this example. A diagram of the switching system is shown in Figure 6 (a) with both output states represented by the solid and dashed arrows, respectively. Recall, the Chatoyant representation of this system is shown in Figure 1. The mirror is 100 x 100 μm, and is positioned at the end of a 700 μm cantilever beam. Both beam and mirror are fabricated with polysilicon, with the gold covered mirror having an ideal reflectivity of 100%. The beam is 2 μm wide and 100 μm thick, while the mirror is 4 μm thick, to ensure the mirror remains rigid. Collimating lenses (f = 50 μm) are placed 50 μm from the fiber ends, and there is a free-space gap of 100 μm between the lenses. The mirror, when in the optical path, is positioned in the center of the free-space gap, 50 μm from each lens.

We first use Chatoyant to analyze the mechanical movement of the beam and mirror. The more significant mode frequencies

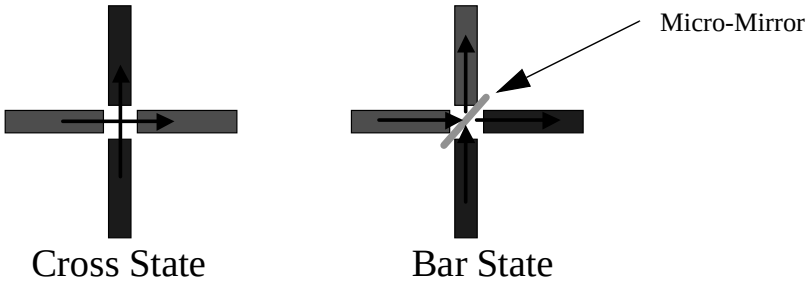

Figure 5: 2x2 Switch: Cross and Bar State

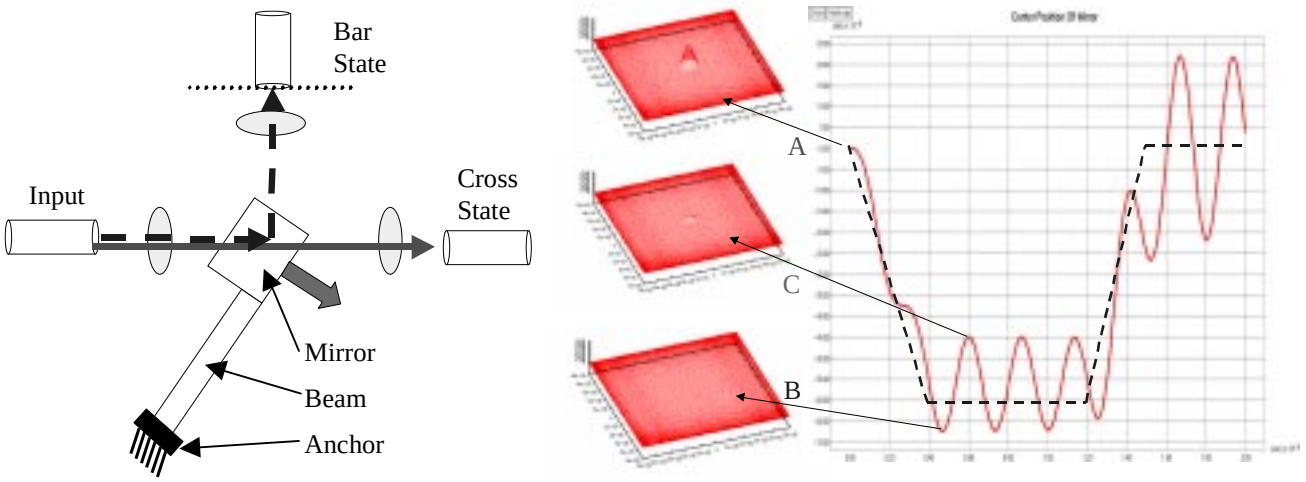

Figure 6: (a) Switching System(b) Mirror Response and Intensity Distributions

of the beam, including the mirror mass, are determined to be 3.7 kHz and 27.1 kHz. These results are within 5% of the solution given from ANSYS. For a switching speed of 400 µsec, the response of the beam, in terms of the center position of the mirror from the original steady-state value, is shown in Figure 6 (b). The switching electro-static force applied to the cantilever beam is also included in Figure 6 (b), represented by the dashed line.

We next examine the optical power that is detected on a 100 µm square observation plane at the bar fiber. Optical intensity distributions at the observation plane are included for three points on the response curve, labeled A, B, and C. A is when the mirror is completely inserted in the optical path, achieving the bar state in the system. B is at the point where the mirror is totally out of the optical path, achieving the cross state. As seen in the intensity distribution, no substantial power reaches the bar fiber observation plane. As the mirror bounces, C is measured as the mirror partially moves back into the optical path, causing some light to be reflected off the mirror and be detected at the bar fiber. However, at this time, the switch is set in the cross state, causing the possibility of crosstalk or the detection of a false "1" on the bar fiber. This problem is further exemplified in Figure 7 (a). This shows a graph of the power detected on the bar fiber end (10 µm diameter) in terms of dB lost. As expected, the power detected corresponds to the mirror position movement seen in Figure 6 (b). With the mirror response, point C has a power loss of only 3 dB at the bar fiber end, resulting in 50% of the power still being detected at the bar fiber.

The three intensity contours for each of the points are seen in Figure 7 (b), along with a circle drawn to represent the fiber end. For case A, the light strikes the mirror in the center and reflects directly into the bar fiber. As seen through Figure 7 (a) and (b), the contour for A is directly on the fiber, and we consider this full detected power (0 dB loss). For case B, the mirror is moved totally out of the optical path, resulting in virtually no power being detected on the fiber (61 dB of loss). However, it is

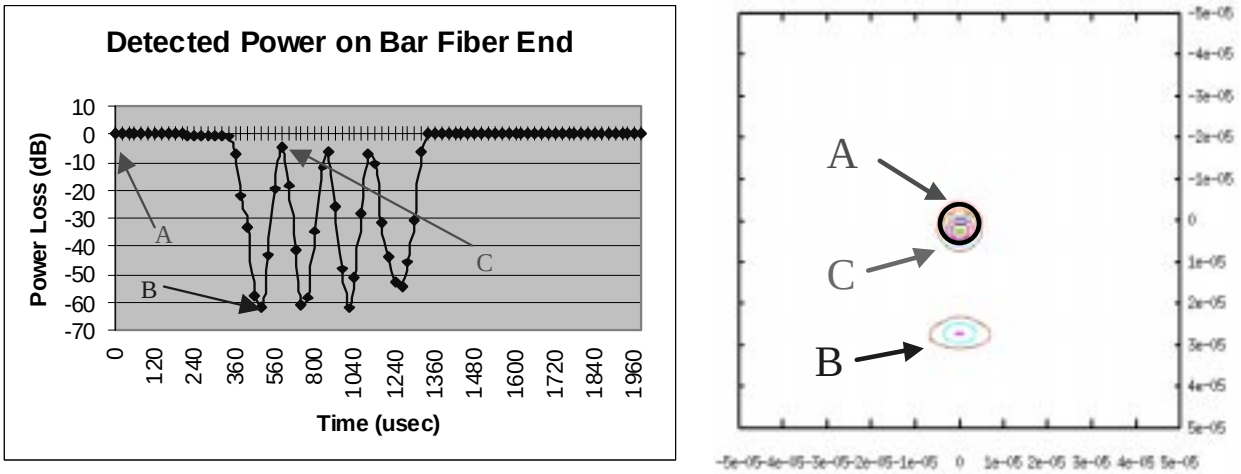

Figure 7: (a)Power Received on End of Bar Fiber (b) Contour Distributions

interesting to note that even though almost no power is received at the fiber end, there is still a diffractive effect, with very low power, striking the observation plane, approximately 28 μm away from the fiber center. In this system, this diffractive effect is not destructive, however, an effect like this could introduce crosstalk in larger scaled systems. For case C, when half the optical beams reflects off the mirror, the power is still concentrated, however, it is centered 3 μm from the fiber center, resulting in a 3 dB loss of power at the bar fiber end. We note that with a slower switching speed, the bounce is not significant, and the system experiences close to zero crosstalk.

7. CONCLUSION AND FUTURE WORK

We have presented a methodology for the simulation of mixed-technology (optical, electrical and mechanical) devices in a system-level simulation framework. The system simulation is a discrete event simulation of piecewise linear signals. However, each electrical or mechanical module in the system is itself a moderate sized non-linear network modeled using a Modified Nodal Analysis formulation and solver, with a switching algorithm to control the switching of regions of operation for the constituent non-linear devices. Unlike previous approaches, these networks are direct representations of the structure of modules without artificial switches or dummy components.

It has been seen that this PWL methodology for the electrical and mechanical signals works well with the Rayleigh-Sommerfeld optical propagation method to model complete optical MEM systems. Our model representations when used in a system-level approach with the addition of an efficient multi-domain simulator can be used as a powerful tool for analysis in both the early and later stages of the design of multi-domain systems. This is because speed vs. accuracy trade-offs in simulation performance can be accomplished either with an increase in the number of PWL regions used to model non-linearity in the devices, the number of grid points used to represent the complex wave function, or with an increase in the sampling rate of the signals in the system. Therefore, design space exploration can be done quickly with simple models, or coarse sampling rates. This can be followed with more accurate simulations based on detailed models and improved accuracy, all within the same simulation environment.

This same methodology, generalized with a formal mathematical definition of dynamic systems in any domain, allows for the integration of multiple domains in a single system. Consequently, additional domains could follow the same general methodology to increase the number of domains supported in a single mixed-technology CAD tool.

ACKNOWLEDGMENTS

We would like to acknowledge the support of NSF grants ECS-9616879 and CCR-9988319.

REFERENCES

1. Abramowitz, M. and Stegun, I. A., editors, *Handbook of Mathematical Functions with Formulas, Graphs, and Mathematical Tables*, (Dover Publications, Inc., New York, 1972).
2. Buck, J., Ha, S., Lee, E.A., Messerschmitt, D., "Ptolemy: a framework for simulating and prototyping heterogeneous systems," *Int. J. Computer Simulation*, Vol. 4, 1994, pp. 155-182.
3. Chen, R.T., Nguyen, H., Wu, M.C., "A High-Speed Low-Voltage Stress-Induced Micromachined 2x2 Optical Switch," *IEEE Photonics Technology Letters*, Vol.11, No. 11, Nov. 1999, pp.1396-1398.
4. Duncan, W. J., *Reciprocation of Triply Partitioned Matrices* (J. Roy. Aeron. Soc., vol. 60, 1956), pp. 131-132.
5. Fan, C., Mansoorian, B., Van Blerkom, D. A., Hansen, M. W., Ozguz, V. H., Esener, S. C., Marsden, G, C, "Digital free-space optical interconnections: a comparison of transmitter technologies," *Applied Optics*, Vol. 34, No. 17, (June 1995), pp. 3103-3115.
6. Feldmann, P., Freund, R. W., "Efficient linear circuit analysis by Padé approximation via the Lanczos process," *IEEE Trans. Computer-Aided Design*, Vol. 14, May. 1995, pp. 639-649.
7. Freund, R. W., and Feldmann, "Reduced-Order Modeling of Large Passive Linear Circuits by Means of the SyPVL Algorithm," *Proceedings of the ICCAD*, Nov. 1996, pp. 280-287.
8. Goodman, J.W., *Introduction to Fourier Optics*, Second Edition (The McGraw-Hill Companies, Inc., 1996).
9. Gupta, R. K., Hung, E. S., Yang, Y. J., Ananthasuresh, G. K., Senturia, S. D., "Pull-in dynamics of electrostatically-actuated beams," *Proc. Solid-state Sensor & Actuator Workshop*, June 1996.
10. Hecht, E., *Optics*, Second Edition (Addison-Wesley Publishing Company, 1987).
11. Kao, R., Horowitz, M., "Timing Analysis for Piecewise Linear Rsim," *IEEE Trans. Computer-Aided Design*, vol. 13, No.

12, 1994, pp. 1498-1512.
12. Kibar, O., Van Blerkom, Fan, C., Marchand, P. J., Esener, S. C., "Small-signal-equivalent circuits for a semiconductor laser," *Applied Optic*s, Vol. 37, No. 26, (Sept. 1998), pp. 6136-6139.
13. Kielowski, R., *Inside SPICE: Overcoming the Obstacles of Circuit Simulation* (New York: McGraw-Hill, Inc., 1994), Chapter 1 and 3.
14. Kurzweg, T.P., Levitan, S.P., Marchand, P.J., Martinez, J.A., Prough, K.R., Chiarulli, D.M., "CAD for Optical MEMS," *Proceedings of the 1999 Design Automation Conference*, New Orleans, LA, June 20-25, 1999, pp.879-884.
15. Kurzweg, T.P., Levitan, S.P., Martinez, J.A., Marchand, P.J., Chiarulli, D.M., "Diffractive Optical Propagation Techniques for a Mixed-Signal CAD Tool," *Optics in Computing (OC2000)*, Quebec City, CA, June 18-23, 2000.
16. Levitan, S.P., Kurzweg, T.P., Marchand, P.J., Rempel, M.A., Chiarulli, D.M., Martinez, J.A, Bridgen, J.M., Fan, C., McCormick, F.B., "Chatoyant: a computer-aided design tool for free-space optoelectronic systems," *Applied Optics*, Vol. 37, No. 26, September, 1998, pp. 6078-6092.
17. Martinez, J.A., "Piecewise Linear Simulation of Optoelectronic Devices with Applications to MEMS", (unpublished MS Thesis, University of Pittsburgh, Department of Electrical Engineering, 2000).
18. MEMSCAP, http://memscap.e-sip.com/
19. Microcosm Technologies, http://www.memcad.com/
20. Morikuni, J. J., Mena, P. V., Harton, A. V., Wyatt, K. W., "The Mixed-technology Modeling and Simulation of Optoelectronic Microsystems," *Journal of Modeling and Simulation of Microsystems*, Vol. 1, No. 1, 1999, pp. 9-18.
21. Mukherjee, T., Fedder, G.K., "Structured Design Of Microelectromechanical Systems," *Proceedings of 34th Design Automation Conference Anaheim, CA*, June 1997, pp. 680-685.
22. Optical Micro-Machines Inc, http://www.omminc.com/
23. Przemieniecki, J. S., *Theory of Matrix Structural Analysis* (McGraw-Hill, New York, New York, 1968).
24. Romanowicz, B., *Methodology for the modeling and Simulation of Microsystems* (Kluwer Academic Publishers, Norwell, Massachusetts, 1998), pp. 24-39.
25. RSoft, Inc., http://www.rsoftinc.com/
26. Saleh, B.E.A., Teich, M.C., *Fundamentals of Photonics* (New York: Wiley-Interscience, 1991).
27. Vandemeer, J. E., "Nodal Design of Actuators and Sensors (NODAS)," (unpublished M.S. Thesis, Department of Electrical and Computer Engineering, Carniege Mellon University, Pittsburgh, PA, 1997).
28. Vlach, J., Singhal K., *Computer methods for circuit analysis and design* (Van Nostrand Reinhold, New York, NY, 1994), Chapter 4 and 12.
29. Wu, M.C., "Micromachining for optical and Optoelectronic Systems," *Proceedings of the IEEE*, Vol. 85, No. 11, November 1997, pp. 1833-1856.
30. Yang, A. T., and Kang, S. M., "iSMILE: A Novel Circuit Simulation Program with emphasis on New Device Model Development," *Proceeding of the 26th ACM/IEEE Design Automation Conference*, 1989, pp. 630-633.